Synthesis of carbon-supported binary FeCo–N non-noble metal electrocatalysts for the oxygen reduction reaction

Li, Shang; Zhang, Lei; Kim, Jenny; Pan, Mu; Shi, Zheng; Zhang, Jiujun

Publisher's version / Version de l'éditeur:
https://doi.org/10.1016/j.electacta.2010.07.020
Electrochimica Acta, 55, 24, pp. 7346-7353, 2010-07-14

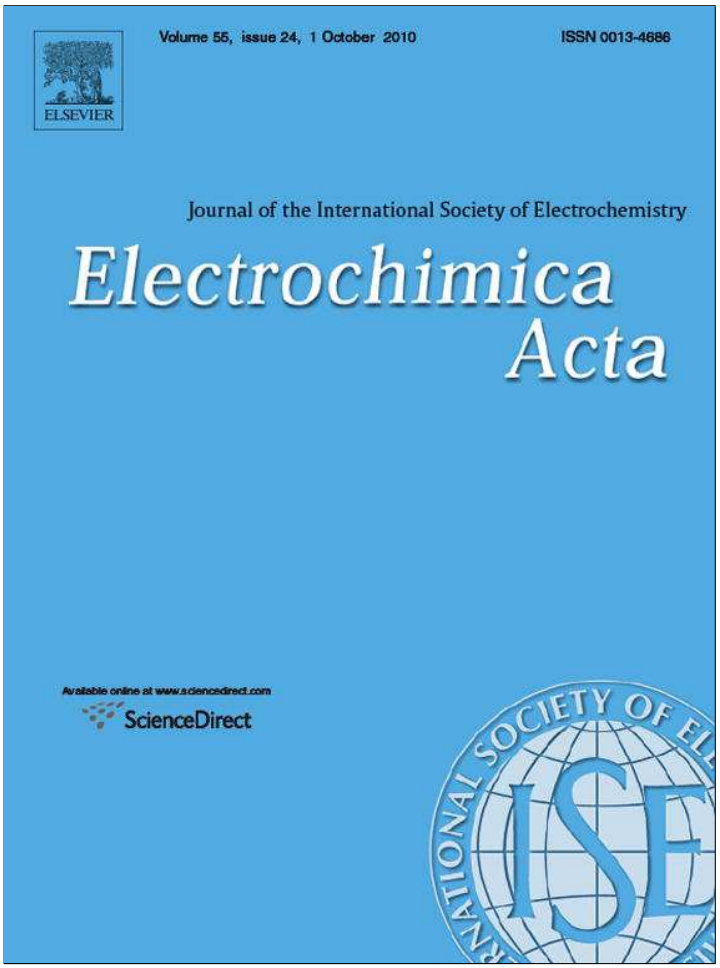

Electrochimica Acta 55 (2010) 7346–7353

Contents lists available at ScienceDirect

Electrochimica Acta

journal homepage: www.elsevier.com/locate/electacta

Synthesis of carbon-supported binary FeCo–N non-noble metal electrocatalysts for the oxygen reduction reaction

Shang Li[a,b], Lei Zhang[a,*], Jenny Kim[a], Mu Pan[b,**], Zheng Shi[a], Jiujun Zhang[a]

[a] Institute for Fuel Cell Innovation, National Research Council of Canada, Vancouver, BC V6T 1W5, Canada
[b] State Key Laboratory of Advanced Technology for Materials Synthesis and Processing, Wuhan University of Technology, Wuhan 430070, PR China

ARTICLE INFO

Article history:
Received 24 June 2010
Accepted 7 July 2010
Available online 14 July 2010

Keywords:
Non-noble metal electrocatalyst
Oxygen reduction reaction (ORR)
Binary iron (Fe)/cobalt (Co)–nitrogen (N)
2,4,6-Tris(2-pyridyl)-1,3,5-triazine (TPTZ)
Proton exchange membrane (PEM) fuel cell

ABSTRACT

In this paper, a carbon-supported binary FeCo–N/C catalyst using tripyridyl triazine (TPTZ) as the complex ligand was successfully synthesized. The FeCo–TPTZ complex was then heat-treated at 600 °C, 700 °C, 800 °C, and 900 °C to optimize its oxygen reduction reaction (ORR) activity. It was found that the 700 °C heat-treatment yielded the most active FeCo–N/C catalyst for the ORR. XRD, EDX, TEM, XPS, and cyclic voltammetry techniques were used to characterize the structural changes in these catalysts after heat-treatment, including the total metal loading and the mole ratio of Fe to Co in the catalyst, the possible structures of the surface active sites, and the electrochemical activity. XPS analysis revealed that Co–N_x, Fe–N_x, and C–N were present on the catalyst particle surface. To assess catalyst ORR activity, quantitative evaluations using both RDE and RRDE techniques were carried out, and several kinetic parameters were obtained, including overall ORR electron transfer number, electron transfer coefficient in the rate-determining step (RDS), electron transfer rate constant in the RDS, exchange current density, and mole percentage of H_2O_2 produced in the catalyzed ORR. The overall electron transfer number for the catalyzed ORR was ~3.88, with H_2O_2 production under 10%, suggesting that the ORR catalyzed by FeCo–N/C catalyst is dominated by a 4-electron transfer pathway that produces H_2O. The stability of the binary FeCo–N/C catalyst was also tested using single Fe–N/C and Co–N/C catalysts as baselines. The experimental results clearly indicated that the binary FeCo–N/C catalyst had enhanced activity and stability towards the ORR. Based on the experimental results, a possible mechanism for ORR performance enhancement using a binary FeCo–N/C catalyst is proposed and discussed.

1. Introduction

Proton exchange membrane (PEM) fuel cells are considered clean energy converting devices because of their high energy density, high energy converting efficiency, and low/zero emissions. Unfortunately, the use of costly Pt-based catalysts, particularly in the PEM fuel cell cathode where the oxygen reduction reaction (ORR) occurs, is hindering commercialization. To reduce the cost of Pt-based electrocatalysts used in PEM fuel cells, lowering Pt loading and/or completely replacing Pt using non-noble metal catalysts have become the goals of intensive research in recent years [1,2]. In light of platinum's scarcity, inefficient recycling, and rising cost, non-noble metal catalysts should be long-term sustainable solutions for PEM fuel cell commercialization.

During the last several decades of research into non-noble metal catalysts, heat-treated Fe- and Co-based nitrogen complexes, including porphyrins, phthalocyanines, dibenzotetraazaanulenes, phenanthrolines, polypyrrole, tripyridyl triazine, and so on have been recognized as the most promising candidates for catalyzing the ORR in an acidic medium [3–9]. It has been found that iron-based complexes can normally catalyze the ORR through a 4-electron reduction pathway to produce water, while cobalt complexes can catalyze a 2-electron reduction pathway [10]. In addition, iron-based catalysts have higher ORR activity than Co-based catalysts but the latter have higher catalytic stability. For example, most recently, Dodelet's group [11] reported a breakthrough in the activity of carbon-supported iron–nitrogen catalyst (Fe–N/C). The volumetric activity of Fe–N/C reached 99 A cm^{-3}, matching that of Pt/C catalyst at a cell voltage of ≥0.9 V and coming close to the 2010 DOE performance target of 130 A cm^{-3} for the ORR on non-noble metal catalysts. Unfortunately, the durability of this Fe–N/C catalyst in a PEM fuel cell was not sufficient. For Co-based catalysts, Zelenay's group at Los Alamos National Laboratory [12] reported that carbon-supported Co–PPY catalyst showed no appreciable drop over 100 h of operation at 0.4 V in an H_2-air

* Corresponding author at: National Research Council Canada, Institute for Fuel Cell Innovation, 4250 Wesbrook Mall, Vancouver, BC V6T 1W5, Canada. Tel.: +1 604 221 3000x5504; fax: +1 604 221 3001.
** Corresponding author. Tel.: +1 604 221 3000x5504; fax: +1 604 221 3001.
E-mail addresses: lei.zhang@nrc.gc.ca (L. Zhang), panmu@whut.edu.cn (M. Pan).

0013-4686/$ – see front matter © 2010 Published by Elsevier Ltd.
doi:10.1016/j.electacta.2010.07.020

fuel cell. In our previous work [13], we employed tripyridyl triazine (TPTZ) as both nitrogen source and Fe complex ligand to synthesize a carbon-supported Fe–N catalyst for the ORR. The performance of this catalyst was close to that of the carbon-supported Co–PPY catalyst developed by Zelenay's group [12]. The overall ORR electron transfer numbers obtained using this Fe–TPTZ-based catalyst were between 3.5 and 3.8, with 10–30% H_2O_2 production, indicating that the Fe–N/C catalyst synthesized in our previous work catalyzed the ORR process mainly through a 4-electron transfer pathway that produced water. Recently, we also synthesized some carbon-supported cobalt tripyridyl triazine (Co–TPTZ) complexes and compared the stability of the resulting catalysts (Co–N/C) after heat-treatment at 700 °C to the stability of our Fe–N/C catalysts [13] under the same conditions. The results indicated that Co–N/C is much more stable than Fe–N/C in an acidic medium. For example, with the Co–N/C catalyst the voltage decreased from 0.778 V to 0.590 V after 115 h of stability testing, at a degradation rate of 1.64 mV h^{-1}. However, with the Fe–N/C catalyst the voltage drop exceeded 20% after 50 h, at a degradation rate of 3.64 mV h^{-1}.

To combine the advantages of high ORR activity and the 4-electron reduction pathway of Fe-based catalysts with the high electrochemical stability of Co-based catalysts, mixed catalysts using Fe and Co as the metal sources have been synthesized by heating mixtures of two transition metal complexes at high temperatures. For example, Jiang and Chu [14,15] synthesized a series of single and binary heat-treated metalloporphyrins (such as HT-CoTPP, HT-FeTPP, and HT-FeTPP/CoTPP) and evaluated their catalytic activity for the ORR. They found that the catalytic activity of binary FeTPP/CoTPP catalysts was much better than that of single CoTPP or FeTPP. The mechanism of this enhanced ORR activity with heat-treated FeTPP/CoTPP binary catalysts has also been explored, and a face-to-face bimetal structure with a specified stereo distance between the two metal centers is believed to favour the 4-electron transfer pathway in the ORR [16]. Dodelet's group [17] also prepared three catalysts by pyrolyzing carbon-supported FeTMPP, CoTMPP, and a mixture of these two metal tetramethoxy porphyrins in an NH_3 atmosphere. The result indicated that (i) the mixed metal catalysts were more active than the single metal catalysts, and (ii) the Co/Fe mixed metal catalyst produced less H_2O_2. Zelenay's group [18] also developed a new ORR binary catalyst with layered "hybrid" materials containing Fe and Co metal centers, polyaniline, and a carbon support. This kind of polyaniline/FeCo/C catalyst showed high ORR activity with selectivity for a 4-electron transfer pathway, producing less than 1% H_2O_2. This catalyst also showed high stability in a hydrogen-air fuel cell.

All of the above-mentioned studies have indicated that heat-treated mixtures of Fe and Co complexes demonstrate enhanced catalytic activity towards the ORR and improved stability in a fuel cell environment, suggesting that Fe/Co–N/C catalysts are promising candidates for the ORR in fuel cells. Thus, more exploration of such binary Fe/Co–N catalysts is necessary to obtain a fundamental understanding of the catalysts structure and active sites, and of the enhancement mechanism.

As part of the continuing effort to develop non-noble metal catalysts for the fuel cell ORR, we designed and synthesized a typical carbon-supported binary Fe/Co–N catalyst to optimize their catalytic activity and stability by combining the advantages of single Fe–N and Co–N catalysts. XRD and EDX techniques were applied to analyze catalyst structure and composition, TEM was used to observe morphology, and XPS was employed to evaluate the electronic structure of the catalyst surface. To characterize the ORR activity, the resulting binary Fe_1Co_1–N/C was coated on a glassy carbon (GC) electrode for electrochemical ORR measurements using cyclic voltammetry (CV), rotating disk electrode (RDE), and rotating ring-disk electrode (RRDE) techniques. For comparison, two single metal-nitrogen catalysts, Fe–N/C and Co–N/C, were also measured under the same experimental conditions.

2. Experimental

2.1. Chemicals

Tripyridyl triazine (TPTZ) (≥98%), $(NH_4)_2Fe(SO_4)_2{\cdot}6H_2O$, and $Co(NO_3)_2{\cdot}6H_2O$ were purchased from Aldrich and used as received. Black Pearls 2000, used as the catalyst support, was purchased from Cabot. Nitrogen gas (N_2) with a purity of 99.999% was purchased from Praxair. All other reagents were analytic grade and used as received without further purification. Deionized water was used to prepare all solutions.

2.2. Catalyst synthesis

In the preparation of the binary Fe_1Co_1–N/C catalysts, the mole ratio of total metal to TPTZ ligand was kept at 1:2.1. During synthesis of 5 wt% Fe_1Co_1–N/C, a metal precursor (an aqueous solution of $Co(NO_3)_2{\cdot}6H_2O$ and $(NH_4)_2Fe(SO_4)_2{\cdot}6H_2O$, with a total metal concentration of 0.0174 M and Fe:Co = 1:1 (mol)) was slowly added under constant stirring into the 0.16 M hydrochloric acid solution containing 0.03657 M TPTZ, forming a black-brown complex. This complex solution was continuously stirred for at least 2 h to allow the complex formation reaction to finish. A carbon suspension was obtained by mixing Black Pearls 2000 with a 3% ethanol solution at 60 °C under constant stirring. To synthesize the carbon-supported Fe_1Co_1–TPTZ complex (Fe_1Co_1–TPTZ/C), the complex solution prepared above was added into the carbon suspension and stirred for at least 20 h. The formed mixture was then dried in an oven at 90 °C overnight to form a black Fe_1Co_1–TPTZ/C powder. The metal content of this powder was expected to be 5 wt%. To remove any residual air, the powder was then placed in a tube furnace under N_2 at a flow rate of 150 mL min^{-1} for 2 h. After that, the tube furnace was adjusted to increase the temperature at a ramping rate of 5 °C min^{-1} until the desired heat-treatment temperature was reached. The furnace was then held at this temperature for 2 h, followed by cooling at a rate of 5 °C min^{-1} until room temperature was reached. The final carbon-supported catalyst (expressed as 5 wt% FeCo–N/C) was thereby obtained. The heat-treatment temperatures were 600 °C, 700 °C, 800 °C, and 900 °C.

2.3. Physical characterization of the catalysts

The average chemical compositions of the Fe_1Co_1–N/C catalysts were determined by EDX analysis (Link Isis System, Oxford). To characterize the catalyst structure, XRD measurements were performed using a Bruker D8 Advance X-ray diffractometer with Cu Kα1 radiation. The XRD patterns were recorded between 0° and 90°, and the powder diffraction file database was used to assign the diffractograms. XPS (Leybold MAX200) was employed for catalyst electronic structure analysis.

2.4. Preparation of the working electrodes

In our prepartion of the working electrode, 10 μL catalyst ink, which consisted of 2 mg catalyst in 1 mL solvent, was pipetted onto the surface of a GC disk electrode (geometric area 0.20 cm^2). The catalyst loading was controlled at 0.1 $mg_{catalyst}$ cm^{-2}. After the coating was dried, 5 μL of Nafion® ionomer solution (1% in alcohol solution) was dropped on top of the catalyst coating to form a catalyst layer.

If the ratios of Fe to Co in the catalyst powders were different, the catalyst layers formed using these different catalyst inks were

Table 1
Metal loadings and molar ratios of Fe/Co to FeCo–N/C catalyst. The target for the total metal loading of Fe + Co in the FeCo–TPTZ complex is 5 wt%.

Catalyst	Heat-treatment temperature (°C)	EDX results in catalyst		Molar ratio (Fe/Co)
		(wt% Fe)	(wt% Co)	
FeCo–N/C	600	2.48	2.68	0.98
	700	2.61	2.75	1.00
	800	2.56	3.08	0.88
	900	3.33	3.69	0.95

expected to have different metal ratios, even though the catalyst loadings were the same.

2.5. Electrochemical measurements

All electrochemical measurements were carried out using a conventional three-compartment electrochemical cell containing a working electrode (GC), coated with an Fe_1Co_1–N/C catalyst layer, a counter electrode (Pt wire), and a reference electrode (a reversible hydrogen electrode (RHE)). The electrolyte was either N_2- or O_2-saturated 0.5 M H_2SO_4. Rotating disk electrode (RDE) and rotating ring-disk electrode (RRDE) techniques were used to perform electrochemical measurements using a multi-potentiostat (Solartron 1480) and a Pine RDE instrument. Cyclic voltammograms (CVs) and single-scan current–voltage curves were collected in the potential range of 0.05–1.0 V (vs. RHE). An RRDE was used to detect hydrogen peroxide during the ORR catalyzed by Fe_1Co_1–N/C. The ring electrode collection efficiency was calibrated at 0.19. The ring potential was fixed at 1.4 V vs. RHE to oxidize any peroxide produced during the potential scan of the disk electrode from 0.05 V to 1.0 V (vs. RHE). As a stability test, the current density was fixed at 3.5×10^{-2} mA cm^{-2} to record the change in voltage over time. All current densities reported in this paper were normalized to the geometric surface area of the disk electrode. All electrochemical experiments were carried out at room temperature and ambient pressure.

3. Results and discussion

3.1. Physical characterization of the Fe_1Co_1–N/C catalysts

In our previous work [19], heat-treated Fe–TPTZ/C or Co–TPTZ with a 3–5% metal loading yielded the best catalytic activity. For a consistent comparison, all catalysts in this paper were prepared using the same metal loading of 5%.

To obtain the real Fe and Co contents of the heat-treated Fe_1Co_1–N/C catalysts, the sample was measured using EDX. The obtained Fe and Co contents and their molar ratios are listed in Table 1. All total metal loadings in the experimental catalysts are greater than 5 wt%, indicating that part of the TPTZ ligand and/or part of the carbon support decomposed and were lost from the catalyst particles during heat-treatment at higher pyrolysis temperatures [20]. The total weight percentage of metal (M = Fe + Co) in the as-prepared Fe_1Co_1–TPTZ/C complex can be expressed as follows:

$$\text{wt\% } M = \frac{W_{Co} + W_{Fe}}{W_{Co} + W_{Fe} + W_{TPTZ} + W_C} \quad (1)$$

where W_{Fe}, W_{Co}, W_{TPTZ}, and W_C are the weights of Fe, Co, TPTZ, and carbon in the sample, respectively. In this experiment, wt% M is 5 wt%. From this Eq. (1), it can be seen that if TPTZ and the carbon support decompose and are lost from the sample, the value of wt% M will increase. The molar ratio of Fe to Co in the FeCo–N/C catalysts is close to 1, indicating that the relative content of the metals does not change after heat-treatment.

For physical characterization, XRD was initially employed to gain insight into the crystalline nature of the 5 wt% Fe_1Co_1–N/C catalyst heat-treated at different temperatures, as shown in Fig. 1.

From Fig. 1 it can be seen that the sample heat-treated at 600 °C exhibits a small peak at 43.5°, which may probably correspond to the metallic Co phase formation. This metallic Co phase could be further confirmed from the XRD pattern when temperature is further increased to or higher than 700 °C, where two sharp, narrow diffraction peaks at 43.9° and 51.2° are clearly observed at the same time. These two peaks can be attributable to typical metallic Co phases (44.2° and 51.5°). When the temperature increases to 900 °C, three new diffraction peaks at 44.8°, 65.5°, and 82.6° are observable and can be attributed to typical metallic Fe phases (44.6°, 65.0°, and 82.3°), suggesting that metallic Fe was formed during heat-treatment due to decomposition of the Fe_1Co_1–TPTZ/C complex. The wide peak at 24° corresponds to the carbon support. Therefore, heat-treatment at temperatures higher than 700 °C could lead to the undesirable decomposition of metal-TPTZ complexes to their metallic state, which might spontaneously oxidize to metallic oxides when exposed to air at room temperature [21]. The decompositions of Fe/Co–TPTZ complexes during heat-treatment are believed to be complicated processes producing many species, including metal-nitrogen species, metals in their metallic state, and metal carbides. Normally, metallic state metals and/or metallic oxides have no catalytic activity towards the ORR; therefore, to avoid the formation of a metallic state in these catalysts, the heat-treatment temperature during Fe_1Co_1–N/C synthesis should not go above 700 °C.

3.2. Surface electrochemistry of Fe_1Co_1–N/C catalysts

To characterize the electrochemical activity of Fe_1Co_1–N/C using surface voltammograms, each catalyst was coated on a GC electrode to form a thin catalyst layer, then immersed in a 0.5 M H_2SO_4

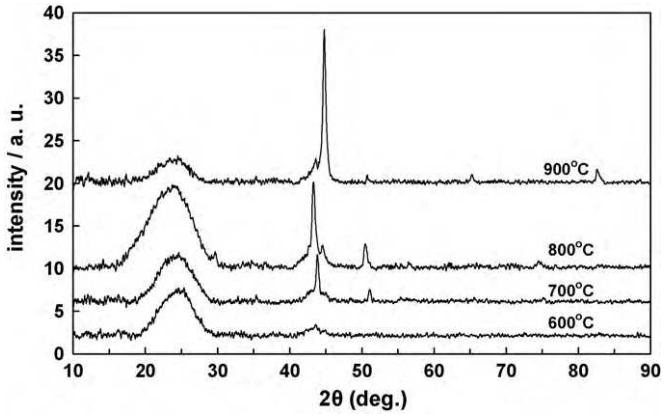

Fig. 1. XRD patterns for Fe_1Co_1–N/C samples after being heat-treated at 600 °C, 700 °C, 800 °C, and 900 °C. Metal loading: 5.0 wt%.

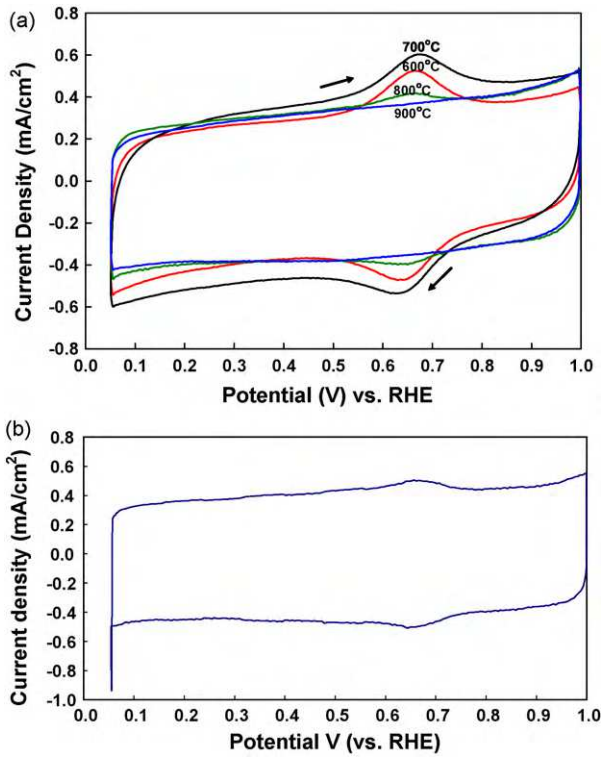

Fig. 2. (a) Cyclic voltammograms of Fe_1Co_1–N/C catalysts heat-treated at 600 °C, 700 °C, 800 °C, and 900 °C. Catalysts were separately coated on a glassy carbon electrode surface. Recorded in N_2-saturated 0.5 M H_2SO_4 solutions. Fe_1Co_1–N/C catalyst loading: 0.1 mg cm^{-2}. Potential scan rate: 50 mV s^{-1}. (b) Cyclic voltammogram of single Fe–N/C catalysts heat-treated at 800 °C. Recorded in N_2-saturated 0.5 M H_2SO_4 solutions. Fe–N/C catalyst loading: 0.1 mg cm^{-2}. Potential scan rate: 50 mV s^{-1}.

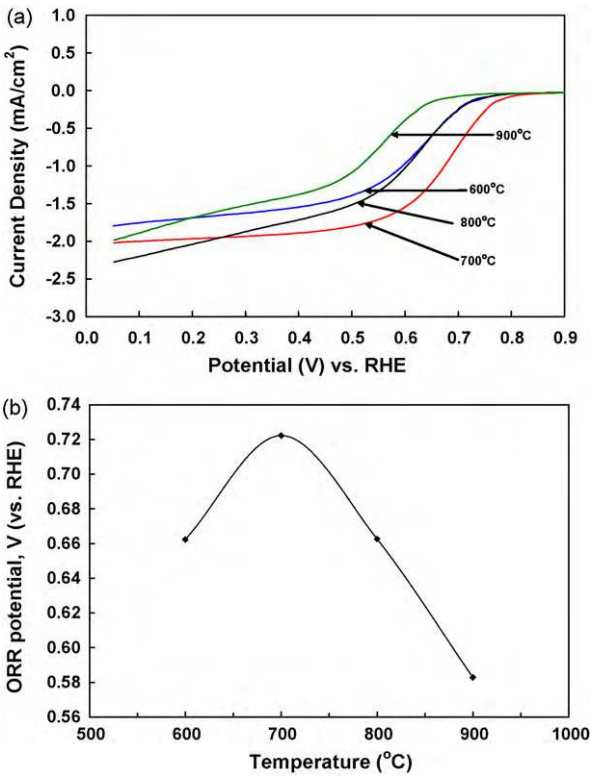

Fig. 3. (a) Current–voltage curves recorded on a rotating glassy carbon electrode coated with different Fe_1Co_1–N/C catalysts obtained after heat-treatment at various temperatures, as marked in the figure. Electrolyte: O_2-saturated 0.5 M H_2SO_4 solution; electrode rotating rate: 400 rpm; potential scan rate: 5 mV s^{-1}; FeCo–N/C catalyst loading in the coating layer: 0.1 mg cm^{-2}. (b) ORR potentials at 0.5 mA cm^{-2} as a function of heat-treatment temperature (data taken from Fig. 5(a)).

electrolyte solution saturated with pure nitrogen. Fig. 2(a) shows cyclic voltammograms of the GC electrode coated with Fe_1Co_1–N/C catalysts obtained at different heat-treatment temperatures, for comparison. A reversible redox wave at about 0.65 V (vs. RHE) is clearly observable. In our previous research on a single Fe–N/C catalyst [22], we recorded a redox wave at the same position and assigned it to a redox process of Fe(II)/Fe(III). The corresponding electrochemical reaction may be expressed as Eq. (2):

$$\text{Fe(II)} \leftrightarrow \text{Fe(III)} + e^- \quad (2)$$

For the single Co–N/C catalyst under at the same experimental conditions, no redox wave was observed, as reported in our previous paper [submitted to Electrochimica Acta], indicating that Co(II) is not active in the electrode potential range under study. Therefore, the redox wave in Fig. 2(a) is believed to be solely from Fe(II)/(III). In addition, the same peak potential positions for both single Fe–N/C (as shown in Fig. 2(b)) and binary Fe_1Co_1–N/C catalysts indicate that in the binary Fe_1Co_1–N/C catalyst, the interaction between Fe ion and Co ion is insignificant. The peak current decreases with increasing heat-treatment temperature until reaching zero at 900 °C, indicating that the density of Fe ion gradually disappeared. This might be due to the formation of iron metallic state, as observed in the XRD measurements (Fig. 1). Of course, the Co ion portion of the FeCo–N/C catalyst should also gradually decrease with increasing heat-treatment temperature, due to the corresponding formation of cobalt metallic state, as observed in Fig. 1. Unfortunately, because Co(I)/(II) is not electrochemically active, the surface electrochemical method could not give any indication of changes in the Co ion density as heat-treatment temperature changed. However, the trend for the loss of Co ion density with increasing heat-treatment temperature should be similar [submitted to Electrochimica Acta].

3.3. ORR activity of Fe_1Co_1–N/C catalyst

To measure the ORR activity of the synthesized Fe_1Co_1–N/C catalyst, the GC electrode coated with it was rotated at 400 rpm in a 0.5 M H_2SO_4 solution containing saturated O_2, then measured using linear scanning voltammetry. The obtained current–voltage curves for catalysts heat-treated at 600 °C, 700 °C, 800 °C, and 900 °C are shown in Fig. 3(a). The optimum catalyst for the ORR was obtained at a heat-treatment temperature of 700 °C. In descending order, the heat-treatment temperatures at which improved ORR catalysts were formed was as follows: 700 °C > 600 °C > 800 °C > 900 °C. This order is consistent with the order of the Fe(II)/Fe(III) redox peak current density, suggesting that Fe ion might play an important role in the catalyzed ORR process. As for the role of Co ion in the ORR, comparison of the catalytic current densities obtained using single Fe–N/C and binary FeCo–N/C catalysts can indicate the contribution of Co ion to catalytic activity. For example, under the same conditions, 5 wt% of binary FeCo–N/C can yield an ORR current density of 1.7 mA cm^{-2} at 0.6 V (vs. RHE), while 5 wt% of single Fe–N/C can only give a current density of 1.2 mA cm^{-2}. This clearly indicates some enhancement effect when part of the Fe is replaced by Co. In a later section of this paper, the enhancement mechanism will be further discussed. For additional comparison, the electrode potentials at 0.5 mA cm^{-2} were plotted as a function of heat-treatment temperature, as shown in Fig. 3(b); again, this indicates that the optimum heat-treatment temperature, resulting in the highest ORR potential, is 700 °C.

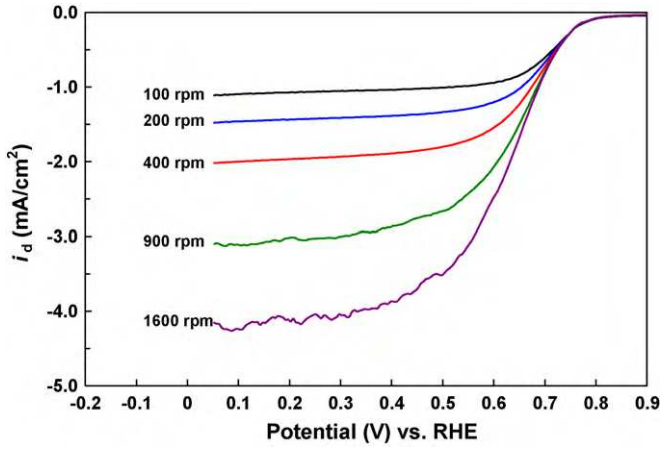

Fig. 4. Current–voltage curves for the ORR on a glassy carbon electrode coated with Fe_1Co_1–N/C catalyst. Recorded in a 0.5 M H_2SO_4 solution at various electrode rotation rates, as marked. Potential scan rate: 5 mV s^{-1}; Fe_1Co_1–N/C loading in the catalyst coating: 0.10 mg cm^{-2}.

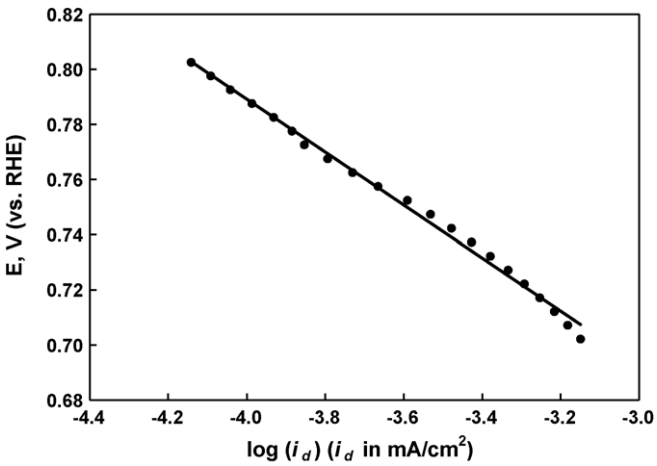

Fig. 5. Tafel plot according to Eq. (3). Data taken from Fig. 4.

3.4. Kinetic parameters derived from the ORR catalyzed by Fe_1Co_1–N/C catalysts

For additional quantitative analysis, both rotating disk electrode and rotating ring-disk electrode techniques were employed to record the current–voltage curves under different conditions. As it is well recognized, these two techniques allow one to quantitatively evaluate kinetic parameters such as overall ORR electron transfer number, electron transfer coefficiency in the rate-determining step (RDS), electron transfer rate constant in the RDS, exchange current density, and the mole percentage of H_2O_2 produced in the catalyzed ORR. The Fe_1Co_1–N/C catalyst used in this section was obtained by heat-treatment at 700 °C, and had demonstrated optimal ORR activity (as shown in Fig. 3). Fig. 4 shows the current–voltage curves recorded at various electrode rotation rates from 100 to 1600 rpm in an O_2-saturated solution.

In Fig. 4 it can be observed that in the potential range of 0.7–0.8 V vs. RHE, the disk current density (i_d) for the ORR is almost independent of the electrode rotation rate, suggesting that the current densities in this narrow potential (or low overpotential) range are purely electrochemical kinetic current densities. However, when the potential is less than 0.7 V, the current density becomes dependent on the electrode rotation rate, suggesting that the current densities in the potential range <0.7 V are affected by both electrochemical kinetic and O_2 diffusion currents. The relationship between the electrode potential and the current density in the low overpotential range (i.e., 0.7–0.8 V) can be expressed as a Tafel equation:

$$E = E^o + \frac{2.303RT}{an_\alpha F}\log(i^o) - \frac{2.303RT}{an_\alpha F}\log(i_d) \quad (3)$$

where α is the electron transfer coefficient in the RDS of the ORR, n_α is the electron transfer number in the RDS (for the ORR process on an electrode, the electron transfer number in the RDS is taken to be 1), E is the applied electrode potential, E^o is the thermodynamic electrode potential under the measurement conditions (E^o = 1.23 V vs. RHE for our experimental conditions), R is the universal gas constant (8.314 J mol^{-1} K^{-1}), T is the temperature (K), and F is Faraday's constant (96,487 C mol^{-1}). Plotting E as a function of $\log(i_d)$, as shown in Fig. 5, the Tafel slope (=2.303$RT/an_\alpha F$) and the intercept (= E^o +(2.303$RT/an_\alpha F$) $\log(i^o)$) can be separately obtained, and then two important ORR kinetic parameters (the electron transfer coefficient, α, and the exchange current density, i^o) can be calculated if E^o, n_α (=1), R, T, and F are known. From the value of i^o, the kinetic rate constant (or electron transfer rate constant) in the RDS, k_e, can be obtained using the relationship $i^o = nFk_eC_{O_2}$ (where the value of n is obtained from averaging the values for overall electron transfer number at different electrode potentials). The obtained values of these parameters are listed in Table 2.

3.5. RRDE measurements to obtain the overall ORR electron transfer number and the amount of H_2O_2 produced

For a quantitative evaluation, the number of electrons transferred and the percentage of H_2O_2 produced during the catalyzed ORR can be calculated using Eqs. (4) and (5), respectively [23]:

$$n = \frac{4i_d}{i_d + (i_r/N)} \quad (4)$$

$$\text{mol\% } H_2O_2 = 100\left(\frac{i_r}{i_d N}\right) \quad (5)$$

where I_d, I_r, and N are the disk current, ring current, and collection efficiency (0.19 in the present work), respectively. Fig. 6 shows the H_2O_2 percentage as a function of the disk electrode potential. The ORR electron transfer number varies in the range of 3.80–3.95, suggesting that the dominant reaction pathway is a 4-electron transfer process from O_2 to H_2O, with only 3–10% H_2O_2 produced.

3.6. Mechanism discussion

3.6.1. Possible catalyst active sites for ORR

In single Fe–N and/or Co–N catalysts for the ORR, the structures of the catalyst active sites after heat-treatment seem to be

Table 2
Electron transfer coefficient α (assuming the electron transfer number n_α in the ORR rate-determining step is 1), exchange current density i^o, electron transfer rate constant k_e, overall ORR electron transfer number, and mole % of H_2O_2 produced in the ORR. Electrolyte: O_2-saturated 0.5 M H_2SO_4 solution; Fe_1Co_1–N/C catalyst loading in the electrode coating layer: 0.10 mg cm^{-2}; temperature: 25 °C.

Electron transfer coefficient, α	Exchange current density, i^o (A cm^{-2})	Electron transfer rate constant in RDS, k_e (cm s^{-1})	Overall ORR electron transfer number	Mole % of H_2O_2 produced in the ORR
0.62	2.6×10^{-9}	6.8×10^{-9}	3.80–3.95	3–10

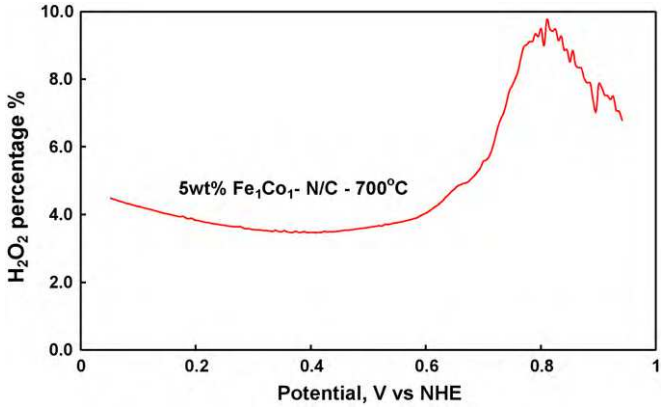

Fig. 6. The corresponding $\%H_2O_2$ produced for the ORR catalyzed by FeCo–N/C catalyst obtained after heat-treatment at 700 °C. Data obtained using rotating ring (Pt)-disk electrode (glassy carbon coated with FeCo–N/C catalyst) in an O_2-saturated 0.5 M H_2SO_4 solution; electrode rotating rate: 1600 rpm; catalyst loading in the disk coating: 0.1 mg cm^{-2}.

complicated and are not yet fully understood. However, several decades of effort have led to the proposal of two kinds of catalyst active sites: one is $M–N_x$ (M = Fe or Co, and x could be 2 or 4) [7], and the other is a C–N group on the carbon support surface, formed by decomposition of the nitrogen-containing ligand [24]. These two kinds of catalyst active sites were observed using XPS in our previous work [13,24]. For heat-treated binary catalysts such as Fe/Co–N, the dominant catalytic sites in addition to the C–N group are thought to be MN_4 cores and the face-to-face structure formed by these cores [15]. In this paper, to have better understanding of the possible catalyst active sites for Fe_1Co_1–N/C, XPS patterns were collected. The XPS narrow-scan spectra for N 1s levels for the Fe_1Co_1–TPTZ/C sample heat-treated at 700 °C are shown in Fig. 7. The N 1s peak can be deconvoluted into two components, centered near the binding energies of 398.74 eV and 401.26 eV, respectively. The N 1s peak at 398.74 eV (N2) may be assigned to a pyridinic-type nitrogen, which consists of an N atom at the edge of a graphene layer, contributing 1-electron to the π bonding, while the 401.26 eV peak (N1) might correspond to the nitrogen on the central aromatic ring in the TPTZ molecule. In particular, the much higher N atomic percentage of 76.9% (N2) compared to 26.1% (N1) indicates that the atomic N contributing to the catalytic activity of Fe_1Co_1–N/C after heat-treating Fe_1Co_1–TPTZ/C at 700 °C might be mainly from pyridinic-type nitrogen (N2) rather than aromatic-type (N1).

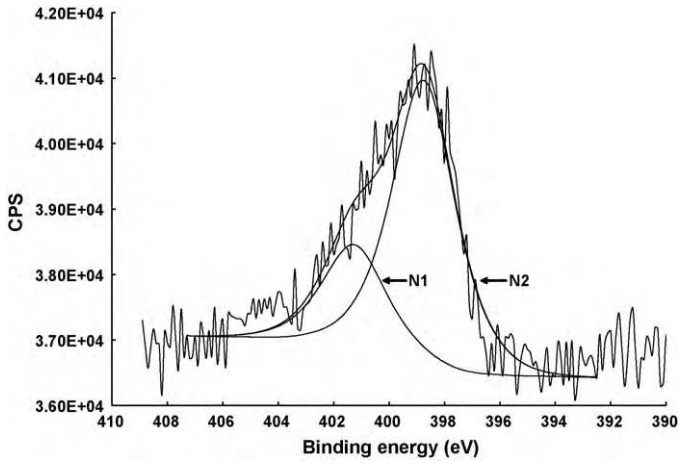

Fig. 7. XPS narrow-scan spectra for N 1s levels; Fe_1Co_1–TPTZ/C sample heat-treated at 700 °C.

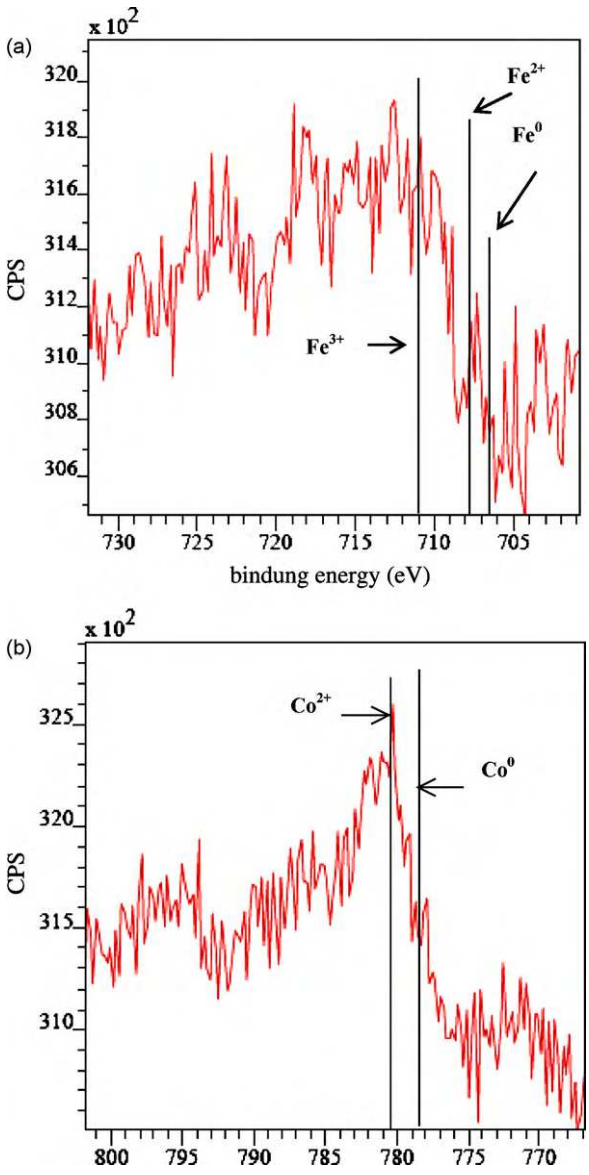

Fig. 8. XPS narrow-scan spectra for: (a) Fe 2p levels, and (b) Co 2p levels; Fe_1Co_1–TPTZ/C sample heat-treated at 700 °C.

Fig. 8 displays the Fe 2p (Fig. 8(a)) and Co 2p (Fig. 8(b)) narrow-scan spectra for the Fe_1Co_1–TPTZ/C sample heat-treated at 700 °C. The standard binding energies for Fe 2p of Fe^0, Fe^{2+}, and Fe^{3+} are 706.7–707.2 eV, 707.1–708.7 eV, and 710.8–711.8 eV, respectively, and the standard binding energies for Co 2p of Co^0 and Co^{2+} are 778.3 eV and 780.4–783.0 eV, respectively. The median values of these energies are displayed in Fig. 8 as vertical lines. It is clear that Fe^{3+} and Co^{2+} are the dominant species on the catalyst particles.

3.6.2. ORR activity enhancement by binary Fe_1Co_1–N/C when compared to single Fe–N/C and Co–N/C catalysts

To investigate the ORR enhancement effect of the binary Fe_1Co_1–N/C catalyst, Fig. 9 shows the ORR current–voltage curves recorded on the electrode coated with three different catalysts – Fe–N/C, Fe_1Co_1–N/C, and Co–N/C – for comparison. It can be seen that binary Fe_1Co_1–N/C has better catalytic activity than both single Fe–N/C and Co–N/C. For example, at an ORR current density of 0.5 mA cm^{-2}, the electrode potentials are 0.453 V, 0.722 V, and 0.684 V for Fe–N/C, Fe_1Co_1–N/C, and Co–N/C, respectively. Note that in Fig. 9, Co–N/C shows a better ORR activity than Fe–N/C at this spe-

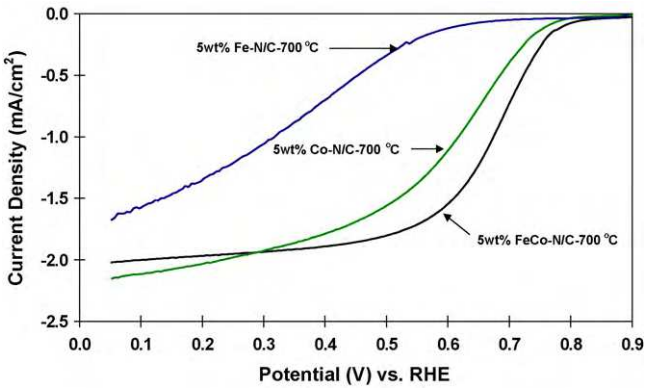

Fig. 9. Linear scanning voltammograms obtained using a rotating glassy carbon electrode coated with Fe–N/C, Fe_1Co_1–N/C, and Co–N/C catalysts, separately. These catalysts were obtained by heat-treating the corresponding metal–TPTZ/C complexes at 700 °C. Electrolyte: O_2-saturated 0.5 M H_2SO_4 solution; electrode rotation rate: 400 rpm; potential scan rate: 5 mV s^{-1}; catalyst loading in the electrode coating layer: 0.1 mg cm^{-2}; metal loading in the catalyst: 5 wt%.

cific heat-treatment temperature (700 °C). However, if the Fe–N/C catalyst is heat-treated at 800 °C (its optimal heat-treatment temperature), its ORR activity is higher than the 700 °C treated Co–N/C. Therefore, it is clear that binary Fe_1Co_1–N/C can have an enhancement effect on ORR activity as compared with single Fe–N/C and Co–N/C. This enhancement effect might be closely related to the replacement of a portion of Co (or Fe) in the single Co–N/C (or Fe–N/C) catalyst by Fe (or Co). Since the weight percentage of total metal in all three catalysts was controlled at the same level, and the mole ratio of Fe:Co in the Fe_1Co_1–N/C catalyst was 1:1, in Fe–N/C, half of the Fe was replaced by Co to form binary Fe_1Co_1–N/C, and in a similar way, in Co–N/C, half of the Co was replaced by Fe to form Fe_1Co_1–N/C. If there is no binary enhancement, the performance of the binary catalyst heat-treated at 700 °C should lie between the plots for Fe–N/C and Co–N/C in Fig. 9.

3.6.3. Proposed ORR enhancement mechanism

Regarding the binary metal catalyst's mechanism, Chu and Jiang [15] have proposed that face-to-face alignment of binary metals, similar to that of dicobalt porphyrin, might be responsible for the observed activity. This type of two-center active site could exist in a mono metal catalyst as well. With the face-to-face alignment of active centers, a direct 4-electron pathway is dominant. The additional benefit of binary metal catalysts is the complementary function each metal exhibits. This model could explain the enhanced activity, even though the exact mechanism is not known. The weakness of this argument is the probability of such a structure forming, given the low metal loading.

Besides this face-to-face binary metal model, the other possibility is a switch center model. The oxygen is reduced to some intermediate at one metal center and released. The intermediate is transferred to another metal center and further reduced to water. For this model to work, parallel ORR reduction pathways with at least one metal center must be involved to some extent. Otherwise, if direct 4-electron pathways were involved for both metal centers, there would be no catalytic interaction between the metal centers and no enhancement. The enhancement is related to the difference between the complementariness of the two metal centers. A good complementary binary catalyst would have one metal center that was very efficient at catalyzing certain reaction steps while the other metal center was efficient at the other steps. These steps include not only electron transfer but also chemical steps like adsorption, desorption, and disproportionation reactions. For the Fe and Co systems that we studied here, it has been shown that the Co system generally has a higher hydrogen peroxide production than the corresponding Fe system. It is well known that without heat-treatment, Co porphyrin and phthalocyanine catalyze a 2-electron ORR, while for Fe, a 4-electron reduction can be catalyzed. A recent study [25] showed that Fe catalyzed the ORR mainly through a 4-electron direct pathway. Fe also has a much higher turnover frequency for the H_2O_2 disproportionation reaction than Co does. Our previous study indicated that Co–N/C catalyst had a mixed 4- and 2-electron mechanism. The electron transfer number was 3.5 and hydrogen peroxide formation was 14%. In the binary catalyst systems, it is possible that there are still some single Co centers that catalyze 2-electron reduction; the hydrogen peroxide produced from these centers could be further reduced at the Fe centers. The possible mechanism for the binary catalyst is illustrated in Fig. 10.

3.7. Evaluation of catalytic stability

To test the stability of the Fe_1Co_1–N/C catalyst, a conventional three-compartment electrochemical cell with O_2-saturated 0.5 M H_2SO_4 solution was used. To control the ORR in a fully kinetic control region, a small current density (3.5×10^{-2} mA cm^{-2}) was used, and the electrode potential change was then monitored. To compensate for the O_2 consumed during the test, the electrode was rotated at 200 rpm. For comparison, samples of 5 wt% Co–N/C and

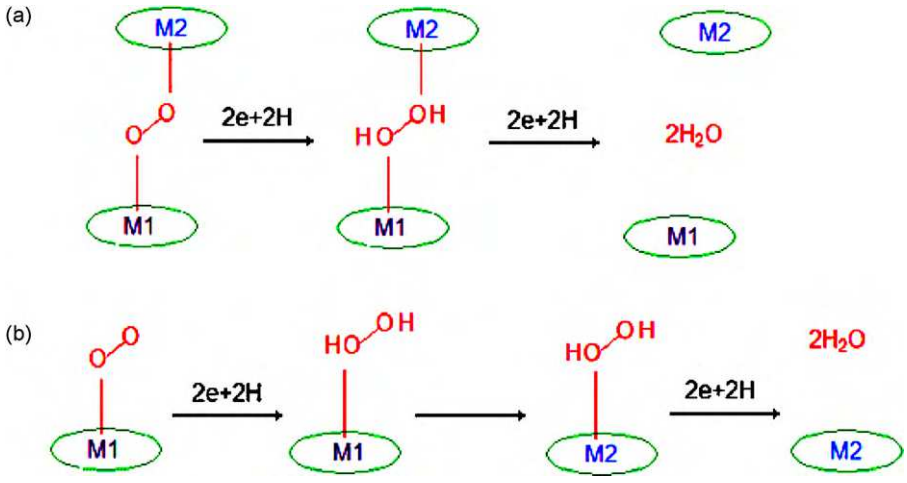

Fig. 10. Schematic of binary mechanism.

5 wt% Fe–N/C were also tested as baseline performances. All catalysts were tested for 140 h, and the obtained degradation rates for Fe–N/C, Co–N/C, and Fe_1Co_1–N/C were 3.4 mV h^{-1}, 1.5 mV h^{-1}, and 1.3 mV h^{-1}, respectively, indicating that binary Fe_1Co_1–N/C is more stable than single Fe–N/C and Co–N/C. These results demonstrated that binary Fe_1Co_1–N/C has not only enhanced ORR activity but also enhanced stability.

4. Conclusion

In this paper, we synthesized a carbon-supported binary Fe_1Co_1–N/C catalyst using tripyridyl triazine (TPTZ) as the complex ligand. The formed Fe_1Co_1–TPTZ complex was then heat-treated at 600 °C, 700 °C, 800 °C, and 900 °C to optimize ORR activity. It was found that 700 °C heat-treatment yielded the most active Fe_1Co_1–N/C catalyst for the ORR. XRD was used to characterize the structural changes in these catalysts after heat-treatment, revealing that when the heat-treatment temperature was at or above 700 °C, the Fe and Co in the Fe_1Co_1–N/C catalyst began to convert to a metallic state. For composition analysis, EDX was used to obtain both the total metal loading and the mole ratio of Fe to Co in the catalyst. XPS analysis revealed Co–N_x and Fe–N_x as well as C–N on the catalyst particle surface. In addition, cyclic voltammetry was used to analyze the electrochemical activity of Fe_1Co_1–N/C. A reversible redox wave near 0.65 V vs. NHE was observed and assigned to the redox process $Fe(III) + e^- \leftrightarrow Fe(II)$. This process is partly responsible for the catalytic activity towards the ORR. To measure the catalysts ORR activity, quantitative evaluation using both RDE and RRDE techniques was carried out, and several kinetic parameters, such as overall ORR electron transfer number, electron transfer coefficient in the RDS, electron transfer rate constant in the RDS, exchange current density, and mole percentage of H_2O_2 produced in the catalyzed ORR, were calculated. The overall electron transfer number for the catalyzed ORR was ~3.88, with H_2O_2 production less than 10%, suggesting that the ORR catalyzed by Fe_1Co_1–N/C was dominated by a 4-electron transfer pathway that produced H_2O. The stability of Fe_1Co_1–N/C was also tested by fixing a current density to record the change in electrode potential over time and comparing the results to those for single Fe–N/C and Co–N/C catalysts under the same conditions. Degradation rates were obtained for these three catalysts, with binary Fe_1Co_1–N/C demonstrating the lowest rate. The experimental results clearly indicated that binary Fe_1Co_1–N/C had enhanced ORR catalytic activity and stability. Based on the experimental results and theoretical calculations, a possible mechanism for ORR performance enhancement by binary Fe_1Co_1–N/C was proposed and discussed.

Acknowledgements

The authors are grateful for the financial support of the Institute for Fuel Cell Innovation, National Research Council of Canada (NRC-IFCI). Professor Shang Li also thanks the China Scholarship Council for its financial support.

References

[1] H.A. Gasteiger, N.M. Marković, Science 324 (3) (2009) 48.
[2] K. Lee, L. Zhang, J. Zhang, J. Power Sources 170 (2007) 291.
[3] R. Jasinski, Nature 201 (1964) 1212.
[4] A. Widelov, Electrochim. Acta 38 (1993) 2493.
[5] G. Lalande, G. Faubert, R. Cote, D. Guay, J.P. Dodelet, L.T. Weng, P. Bertrand, J. Power Sources 61 (1996) 227.
[6] F. Jaouen, M. Lefevre, J.P. Dodelet, M. Cai, J. Phys. Chem. B 110 (2006) 5553.
[7] C.W.B. Bezerra, L. Zhang, K. Lee, H. Liu, A.L.B. Marques, E.P. Marques, H. Wang, J. Zhang, Electrochim. Acta 53 (2008) 4937.
[8] C.W.B. Bezerra, L. Zhang, H. Liu, K. Lee, A.L.B. Marques, E.P. Marques, H. Wang, J. Zhang, J. Power Sources 173 (2007) 891.
[9] G. Faubert, R. Côté, J.P. Dodelet, M. Lefèvre, P. Bertrand, Electrochim. Acta 44 (1999) 2589.
[10] L. Zhang, J. Zhang, D.P. Wilkinson, H. Wang, J. Power Sources 156 (2006) 171.
[11] M. Lefèvre, E. Proietti, F. Jaouen, J.P. Dodelet, Science 324 (3) (2009) 71.
[12] R. Bashyam, P. Zelenay, Nature 443 (2006) 63.
[13] C.W.B. Bezerra, L. Zhang, K. Lee, H. Liu, J. Zhang, Z. Shi, A.L.B. Marques, E.P. Marques, S. Wu, J. Zhang, Electrochim. Acta 53 (2008) 7703.
[14] R. Jiang, D. Chu, J. Electrochem. Soc. 147 (12) (2000) 4605.
[15] D. Chu, R. Jiang, Solid State Ionics 148 (2002) 591.
[16] J.P. Collman, P. Denisevich, Y. Konai, M. Marrocco, C. Koval, F.C. Anson, J. Am. Chem. Soc. 102 (1980) 6027.
[17] M.A. Grigoriu, D. Villers, F. Jaouen, J.P. Dodelet, Proceedings—Electrochemical Society PV 2005-11, 242, 2005.
[18] G. Wu, Z. Chen, K. Artyushkova, F.H. Garzon, P. Zelenay, ECS Trans. 16 (2) (2008) 159.
[19] L. Zhang, K. Lee, C.W.B. Bezerra, J. Zhang, J. Zhang, Electrochim. Acta 54 (2009) 6631.
[20] M. Lefèvre, J.P. Dodelet, P. Bertrand, J. Phys. Chem. B 106 (2002) 8705.
[21] D.A. Scherson, S.L. Gupta, C. Fierro, E.B. Yeager, M.E. Kordesch, J. Eldridge, R.W. Hoffman, J. Blue, Electrochim. Acta 28 (1983) 1205.
[22] L. Zhang, C. Song, J. Zhang, H. Wang, D.P. Wilkinson, J. Electrochem. Soc. 152 (12) (2005) A2421.
[23] U.A. Paulus, T.J. Schmidt, H.A. Gasteiger, R.J. Behm, J. Electroanal. Chem. 495 (2001) 134.
[24] K. Lee, L. Zhang, H. Lui, R. Hui, Z. Shi, J. Zhang, Electrochim. Acta 54 (2009) 4704.
[25] F. Jaouen, J.P. Dodelet, J. Phys. Chem. C 113 (2009) 15422.